available at www.sciencedirect.com

ScienceDirect

journal homepage: www.ejconline.com

Diffusivity and distribution of vinblastine in three-dimensional tumour tissue: Experimental and mathematical modelling

Szabolcs Modok[a], *Philip Hyde*[b], *Howard R. Mellor*[a], *Tiina Roose*[b], *Richard Callaghan*[a,*]

[a]*Oxford Drug Resistance Group, Nuffield Department of Clinical Laboratory Sciences, John Radcliffe Hospital, University of Oxford, Headley Way Headington, Oxford OX3 9DU, UK*

[b]*Oxford Centre for Industrial and Applied Mathematics and Centre for Mathematical Biology, Mathematical Institute, University of Oxford, 24-29 St Giles', Oxford OX1 3LB, UK*

ARTICLE INFO

Article history:
Received 2 February 2006
Received in revised form
24 April 2006
Accepted 2 May 2006
Available online 9 August 2006

Keywords:
Multicellular resistance
Colon cancer
3-D tumour model
Multicell layer
Vinblastine
Diffusion
Mathematical modelling

ABSTRACT

The distribution of chemotherapeutics in solid tumours is poorly understood and the contribution it makes to treatment failure is unknown. Novel approaches are required to understand how the three-dimensional organisation of cancer cells in solid tumours affects drug availability. Since convective drug transport is limited by increased interstitial pressure in poorly vascularised cancers, the aim of this study was to measure the diffusive hindrance exerted by solid tumour tissue. Multicell layer tumour models comprising DLD1 colon cancer cells were characterised and fluxes were determined for [^{3}H]-vinblastine and [^{14}C]-sucrose. The mathematical models provided the diffusion coefficients for both compounds and predicted higher exposure of cells in the vicinity of vessels. The diffusion of vinblastine was three times slower than that of sucrose. Although slow diffusion delays vinblastine penetration into the avascular regions of tumours, the proliferating cells are generally in the marginal area of tumours. The mathematical model that we have developed enabled accurate quantification of drug pharmacokinetic behaviour, in particular, the diffusivity of vinblastine within solid tissue. This mathematical model may be adapted readily to incorporate the influence of factors mediating pharmacokinetic drug resistance.

1. Introduction

Cancer cells evade chemotherapy in many different ways. Research into drug resistance mechanisms is an important driving force for development of anticancer drugs. Since the dawn of chemotherapy in the 1940s, many cellular resistance mechanisms have been observed, yet there are only a few agents capable of 'disarming' these mechanisms. Solid tumours display not only inducible unicellular mechanisms (e.g. efflux pumps) to escape cytotoxic effects but a number of inherent properties that confer resistance. The inherent, or multicellular resistance (MCR), is produced by high cell density and extensive cell–cell contact in the three-dimensional (3-D) arrangement of cancer cells. These factors ensure slow penetration of chemotherapeutics through the solid tumour.[1,2] Despite neo-angiogenesis, the intercapillary distance in tumours remains greater than that observed in normal tissues.[3] In addition, the blood flow in these new and irregularly formed vessels is often turbulent or intermittent.[4] Inadequate vascularisation results in increased interstitial pressure due to decreased drainage of extracellular fluids.[5] The decreased filtration pressure renders diffusion down the concentration

* *Corresponding author:* Tel.: +44 1865 221110; fax: +44 1865 221834.
E-mail address: richard.callaghan@ndcls.ox.ac.uk (R. Callaghan).
0959-8049/$ - see front matter
doi:10.1016/j.ejca.2006.05.020

gradient as the major driving force of drug penetration through the avascular tumour regions.

The tumour spheroid (TS) model of avascular regions of solid tumours has been applied to investigate the distribution of drugs and novel compounds.[6,7] However, quantification of data from experiments with TS is difficult to achieve and the multicell layer (MCL) model, which comprises several layers of cancer cells grown on a semiporous membrane within a cylindrical culture well insert[8] is better suited to measure flux of chemotherapeutics.[2,9,10] The route for drug transport in MCL is mainly extracellular, and this can be hindered by several factors including cellular uptake.[11,12] and metabolism of drugs.[10] However, the flux kinetics have only been analysed in detail for tirapazamine. Therefore, vital information about the relative contributions of diffusivity, convection, cellular uptake and metabolism to intra-tumoural drug kinetics is still missing. Mathematical modelling can facilitate the dissection of penetration/flux kinetics and allow the description of processes with widely applicable parameters, such as the diffusion coefficient.

Vinca alkaloids are strictly cell cycle-specific anticancer drugs that act by slowing the dynamics of microtubule polymerisation.[13] Despite their wide usage, there is little information available on their pharmacokinetic properties within tumour tissue. It is well established that following intravenous administration, vinblastine has a large volume of distribution, suggesting rapid absorption of the drug into the tissues. In contrast, vinblastine was the slowest of a panel of cytostatic drugs to pass through the MCL model of solid tumours.[2] The multidrug efflux pump P-glycoprotein (P-gp or ABC^{B1}) is known to limit the efficacy of vinblastine.[14] P-gp is an ABC transporter, whose expression has prognostic value in many cancers.[15] Inhibition of P-gp was shown to increase accumulation of P-gp substrates in deeper layers of spheroids[7] and to decrease penetration of doxorubicin through MCL.[12] However, the cell lines used in these investigations had been selected for high-level P-gp expression, while clinical samples from drug-resistant tumours are believed to display considerably lower expression.[16] Consequently, a long-standing debate on the precise contribution of P-gp in affecting drug distribution in solid tumours in vivo remains unresolved. Numerous investigations have demonstrated that the expression of P-gp is most prevalent in the deeper layers of TS that are known to display: (i) an altered microenvironment; and (ii) insensitivity to chemotherapeutic drugs.[17]

The aim of the present investigation was to provide detailed flux constants for vinblastine through DLD1 MCL that have P-gp expression levels relevant to human tumour samples. The flux of sucrose was determined to provide a measure of exclusively interstitial diffusion and validate the models. Furthermore, the measured diffusivity of vinblastine was used to estimate its tissue distribution.

2. Materials and methods

2.1. Materials

[^{3}H]-vinblastine sulphate (10.8 Ci/mmol) and [U-^{14}C]-sucrose (601–660 Ci/mol) were purchased from Amersham Biosciences (Little Chalfont, United Kingdom (UK)). [^{3}H]-vinblastine was prepared in methanol and the final solvent concentration was kept below 1% in each experiment. Twenty-four-well culture plates and Transwell-Col inserts (polystyrene sidewall, 6.5 mm internal diameter, bovine placental collagen type I and III coated polytetrafluoroethylene (PTFE) membrane, 0.33 cm^2 surface, 400 nm average pore size) were from Corning Life Sciences (Schiphol-Rijk, The Netherlands). Penicillin and streptomycin were from Cambrex Bioscience (Verviers, France), spinner flasks were from Techne Ltd (Cambridge, UK). All other cell culture materials were from Invitrogen (Paisley, UK). OCT, haematoxylin and eosin were from RA Lamb (Eastbourne, UK). Agarose was purchased from BioWhittaker Biological Applications (Rockland, ME, United States of America (USA)), and Ready Protein + scintillation fluid was from Beckman Coulter Inc. (Fullerton, CA, USA). Benzamidine, leupeptin and pepstatin were from Calbiochem (Merck Biosciences, Nottingham, UK). ECL Western Blotting Detection Kit was from Amersham Biosciences (Little Chalfont, UK). The C219 anti-human P-gp antibody was purchased from CIS (Gif-Sur-Yvette, France), MIB1 anti-Ki67 antibody and Aquamount were obtained from DAKOCytomation (Ely, UK), MACH2 horse-radish peroxidase labelled anti-mouse secondary antibody was bought from Biocare Medical (Concord, USA) and DAKO Peroxidase blocking reagent was from DAKO Corporation (Carpintier, USA). RLT buffer and DNase were from Qiagen (Crawley, UK). Biorad DC protein assay kit was purchased from Biorad (Hercules, USA). All other chemicals were at least analytical grade and were purchased from Sigma.

2.2. Cell lines and MCL culture

Caco2, $MCF7^{WT}$, NCI/ADR^{Res} and DLD1 cells were cultured as monolayers according to American Type Culture Collection (ATCC) and previously published protocols.[14,18] To generate MCL, DLD1 cell monolayers were detached from culture flasks with trypsin/EDTA and 3×10^5 cells were seeded into Transwell-Col inserts. After a few hours the cells had settled and the inserts were transferred into spinner flasks with 50 ml RPMI 1640 medium per insert. Half of the medium was refreshed every third day until the MCL were harvested.

2.3. Morphological characterisation of MCL

MCL were fixed in 4% buffered paraformaldehyde and 4% agarose was layered on both sides to prevent folding of the MCL during subsequent processing. To facilitate the orientation during wax embedding, MCL were cut out from the insert and cast into agarose blocks in the base of a square plastic cuvette. MCL were dehydrated through routine histological processing, embedded in paraffin wax and 5 μm sections were cut. Sections were allowed to dry overnight and stained with haematoxylin and eosin to assess general morphology. The thickness of MCL and the PTFE membrane on cross-sections was measured with a calibrated eyepiece graticule.[18]

2.4. Detection of proliferating cells by Ki-67 immunohistochemistry

Paraffin sections of MCL were dewaxed and, after antigen retrieval (30 s at 120 °C in 10 mM Tris, 1 mM Na_2EDTA, pH 9.0

buffer), stained for Ki-67.[19] Briefly, the slides were incubated for 15 min at room temperature with DAKO peroxidase blocking reagent in a humidified chamber. To reduce non-specific binding, slides were incubated for 30 min in PBST (phosphate buffered saline (PBS) supplemented with 0.1% Tween-20) with 1% bovine serum albumin (BSA). The sections were incubated for 1 h with the MIB1 mouse antibody in PBST with 1% BSA, then for 1 h with an horse-radish peroxidase (HRP)-labelled anti-mouse secondary antibody (MACH 2). Signal was then developed with 3,3′-diaminobenzidine chromogen. Nuclei were counterstained with haematoxylin, and sections were mounted in Aquamount.

2.5. Detection of mdr1 mRNA expression by real-time quantitative TaqMan RT-PCR

Trypsinised DLD1, Caco2, MCF7^{WT} and NCI/ADR^{Res} cells from monolayer cultures were resuspended in RLT buffer containing 1% β-mercaptoethanol and total mRNA extracted according to RNeasy Mini protocol from Qiagen. The residual DNA was digested on the column with DNase. Levels of mdr1 mRNA were quantified by real-time quantitative TaqMan RT-polymerase chain reaction (PCR) using the ABI Prism 7700 Sequence Detection System, Sequence Detector v1.6.3 software (Applied Biosystems, Warrington, Cheshire, UK). The following oligonucleotides were designed with Primer Express Software version 1.0 (Applied Biosystems) and were a gift from Dr Steve Hyde (NDCLS, University of Oxford, UK): forward mdr1 primer, TGG TTC AGG TGG CTC TG; reverse mdr1 primer, CTG TAG ACA AAC GAT GAG CTA TCA CA; FAM labelled mdr1 probe, AGG CCA GAA AAG GTC GGA CCA CCA. 18S rRNA was quantified as the endogenous control using the following oligonucleotides: forward rRNA primer, CGG CTA CCA CAT CCA AG GAA; reverse rRNA primer, GCT GGA ATT ACC GCG GCT; VIC-labelled rRNA probe, TGC TGG CAC CAG ACT TGC CCT C. To match expected expression levels, 100 ng total RNA for mdr1 mRNA and 5 ng for rRNA was reverse transcribed. Subsequently, each sample was subjected to TaqMan PCR according to previously published protocols.[20] Relative expression levels were calculated using the $\Delta\Delta C_T$ method.

2.6. Detection of P-gp protein expression in DLD1 monolayer cultures and MCL by Western blotting

Both monolayer and MCL cultures of DLD1 cells were briefly trypsinised and lysed in phosphate buffered saline (PBS) with 2% sodium dodecyl sulphate (SDS) and protease inhibitors (1 mM benzamidine, 20 μM leupeptin and 1 μM pepstatin). Total protein concentration was determined using the Biorad DC protein assay kit and P-gp expression was detected by Western blotting as described previously[21] using purified P-gp from CHO^{B30} cells as a positive control.

2.7. Determination of flux of radiolabelled compounds through MCL

Inserts with MCL were transferred into 24-well plates with 1 ml fresh medium in the wells (Fig. 1). When the insert was moved to a new well, the medium in the donor compartment (DC) was replaced by 150 μl of fresh RPMI 1640 medium containing [^{14}C]-sucrose and [^{3}H]-vinblastine-sulphate. An agarose overlay has been used previously in DC to eliminate convection in a floating insert,[2,11,12] however, the presence of agarose in the DC can slow down diffusion.[10] The present experimental set-up was able to eliminate convective terms since the insert was kept stable in the culture well and fluid levels in the two compartments were equal, thus resulting in zero fluid pressure gradients (and therefore no convection) across the MCL. Standard MCL culture conditions were maintained throughout the investigations to minimise hydrostatic head or temperature gradient driven convection. At specific times during the assay, the insert was moved to a new well with fresh culture medium, which could potentially induce some convective disturbance.[22] However, the timescale of these events is very short compared with the length of the transport assay, therefore they are unlikely to influence our measurements. To measure the flux of the compounds from the DC through the MCL, 800 μl samples were taken from each of the used wells. The amount of radiolabelled compound was determined by liquid scintillation counting after the addition of 4 ml Ready Protein+ scintillation liquid.

2.8. Non-specific binding of radiolabelled compounds to the plastic of the transport apparatus

Binding to polystyrene can confound flux values. The interaction between polystyrene and radiolabelled compounds can be defined as non-specific binding (NSB), i.e. non-saturable and linear with respect to drug/ligand concentration.[23] Consequently, the proportions of bound and free drug could be estimated at a single drug concentration for the present experimental set-up. The NSB of compounds to the lower chamber was measured by incubating the plastic inserts in wells of a 24-well culture plate in medium containing a 9:1 ratio of cold and radiolabelled compounds. Two hours later, samples were taken from the receiver compartment (RC) and the amount of drug that remained in the culture medium was determined by liquid scintillation counting.

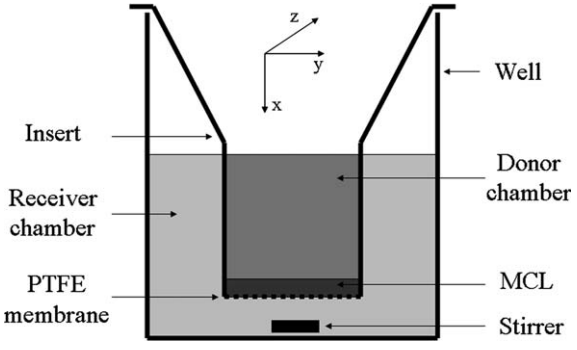

Fig. 1 – The experimental set-up for the drug transport assay is illustrated on a cross-section of a well on a 24-well plate with the insert. The donor and receiver chambers are separated by the polystyrene wall of the cylindrical insert and the membrane with or without the multicell layer (MCL).

2.9. *Measuring the mass transfer coefficient and relative porosity of the collagen-coated PTFE membrane for [^{14}C]-sucrose and [^{3}H]-vinblastine*

The PTFE membrane may itself impede flux of radiolabelled compounds through the MCL system. Consequently, the transport of radiolabelled compounds through the membrane was measured using the same experimental setup shown in Fig. 1, but in the absence of the MCL. The amount of compound transported was determined by scintillation counting after 5, 10, 15, 20, 25 and 30 min incubation using the same set of inserts and adding fresh stock solution of the drug-containing medium. During data analysis the membrane was assumed to be semiporous with negligible thickness.

2.10. *Data analysis*

Data presented are mean ± standard deviation (SD), with the exception of flux data, which was mean ± the standard error of the mean (SEM). Data were analysed with two-tailed Student's t-test using GraphPad Prism 3.2 software and $P < 0.05$ was considered statistically significant. Flux data were analysed with programs written with Matlab 7.0.1 software based on the mathematical models described in the Appendix.

3. Results

3.1. *Growth of MCL from DLD1 cells and their morphology*

DLD1 colon adenocarcioma cells were grown in polystyrene inserts on bovine collagen type I and II coated porous PTFE membranes that allow movement of small molecules, but prevent cells from traversing the membrane. The thickness of the PTFE membranes was measured on cross-sections by an eyepiece graticule and it was 38 ± 1 μm. A minimum of 3×10^5 DLD1 cells were required to fully cover the PTFE membrane as a confluent monolayer. As shown in Fig. 2 the MCL grew exponentially from 24.3 ± 5.7 μm on day 2. Eventually the growth rate slowed down and the MCL reached a thickness of 172 ± 9 μm by the 14th day of culture.

The MCL generated by DLD1 cells displayed much of the cellular heterogeneity found in solid tumours. The cells close to the PTFE membrane had large cigar shaped nuclei, while in those towards the 'upper' surface the nuclei gradually became flattened (Fig. 3(a)). The distribution of proliferating cells also displayed temporal and spatial heterogeneity in MCL. At early stages of MCL growth, the proliferative cells were found throughout the tissue (data not shown). At later stages of the growth curve, the non-proliferating cell mass (Q-cells) appeared in the central region of the MCL (Fig. 3(b)).

3.2. *mdr1 mRNA and P-gp expression in MCL*

It is well established that P-gp is expressed by normal colon epithelial cells and this expression is retained after malignant transformation. [24] P-gp can restrict the cellular uptake of anticancer drugs, such as vinblastine in the TS model.[7] Consequently, it was necessary to characterise expression levels of P-gp in MCL grown from colon carcinoma cells. The mdr1 mRNA levels of DLD1 cells were compared with cells known to express low (MCF7^{WT}), intermediate (Caco2) and high (NCI/ADR^{Res}) levels of P-gp. As shown in Fig. 4(a), DLD1 cells expressed levels of mdr1 mRNA intermediate between the Caco2 and NCI/ADR^{Res} cell lines. This mRNA expression was manifest as measurable expression of the protein product (P-gp) that was marginally higher when the DLD1 cells were grown as MCL (Fig. 4(b)).

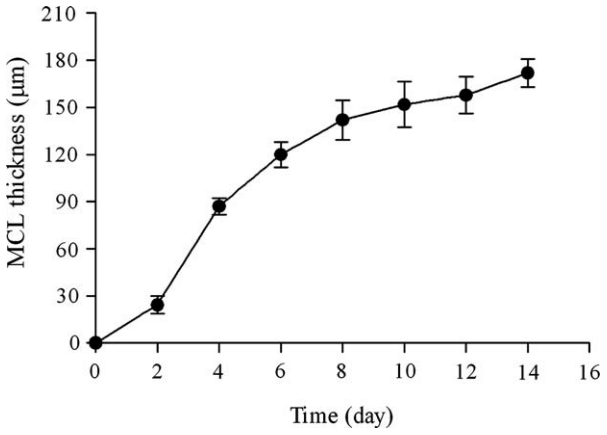

Fig. 2 – Growth of multicell layers was determined by seeding 3×10^5 DLD1 cells into several inserts and subsequent culture in spinner flasks. On specific days, multicell layer (MCL) was harvested and processed as described in the Materials and methods sections. The thickness of haematoxylin and eosin stained cross-sections was measured by a calibrated eyepiece graticule of a light microscope. The data points are mean ± SD of several measurements along several cross-sections of at least 2 MCL.

3.3. *Mass transfer coefficient and relative porosity of the membrane*

The DC and RC were separated by the polystyrene sidewall of the insert and by the collagen-coated PTFE membrane in the absence of MCL in the two-compartment system (Fig. 1). The fluids were levelled in the two compartments when 150 μl and 1000 μl media were loaded in the DC and RC, respectively. The flux of radiolabelled compounds between the two compartments is hindered not only by MCL but also by the PTFE membrane. In order to quantify the membrane's relative porosity, the diffusivity of the radiolabelled compounds in the culture medium must be ascertained. The diffusivity of sucrose in aqueous solution at 25 °C has previously been measured[25] and this value was extrapolated to 37 °C using the Stokes–Einstein equation (7.0×10^{-6} cm^2 s^{-1}). [26] The diffusivity of vinblastine (3.28×10^{-6} cm^2 s^{-1}) was estimated from its molecular radius using the Stokes-Einstein equation as detailed in Table 1. The non-specific binding (NSB) of compounds to the experimental apparatus, is an acknowledged, and yet often ignored, problem in transport systems.[11] Consequently, the NSB of [^{14}C]-sucrose and [^{3}H]-vinblastine to the polystyrene wall of the RC was determined at concentrations used in the transport assay. After 2 h 10.9 ± 1.3% ($n = 3$) and 31.2 ± 1.7% ($n = 3$) of the administered [^{14}C]-sucrose and [^{3}H]-vinblastine were bound, respectively. The measured

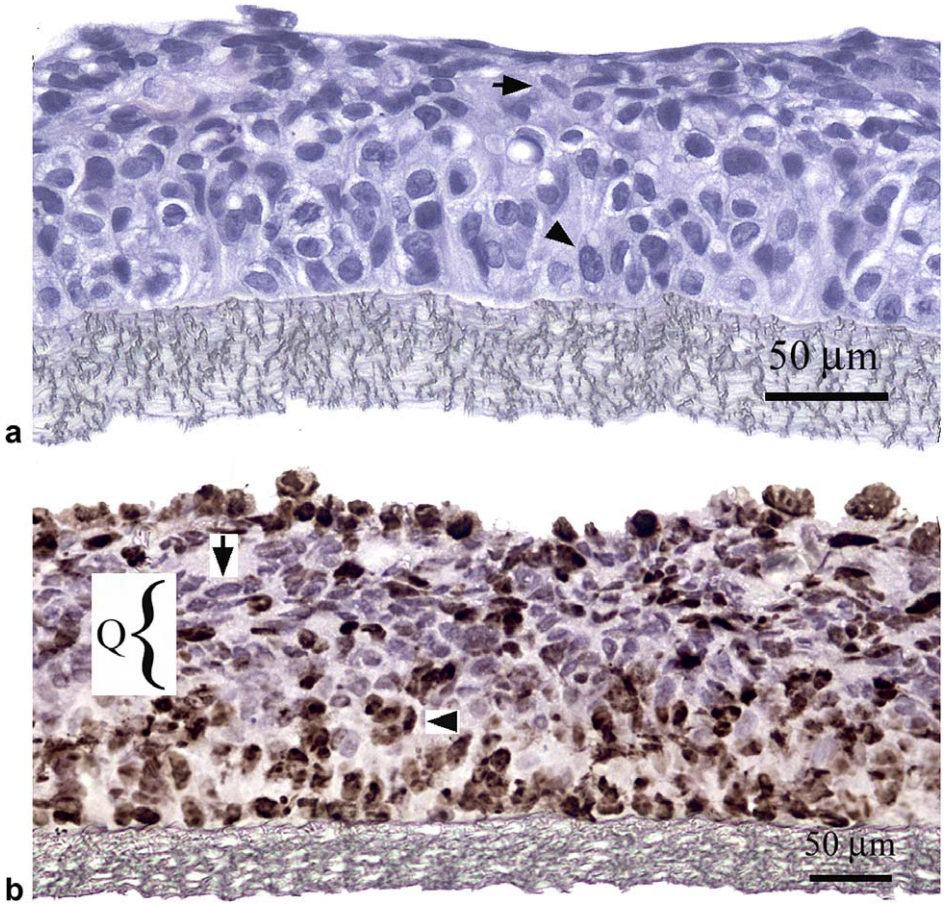

Fig. 3 – Cellular morphology and proliferation in DLD1 multicell layers was studied on 5 μm paraffin sections, which were stained with either (a) haematoxylin and eosin (H & E) or (b) Ki-67 expression detected by immunohistochemistry. Arrows indicate cells with (a) different nuclear morphology and (b) Ki-67 staining. Q indicates the quiescent area of the multicell layer (MCL).

amount of the radiolabelled compound in the RC was corrected with the NSB for all estimations of drug flux through the MCL. The appearance of the two labelled compounds in the RC was measured (CR) over a 30 min period (Fig. 6(a)). Applying the mathematical model described in the Appendix generated values of $1.4 \pm 0.3 \times 10^{-4}$ cm s^{-1} as the mass transfer coefficient for sucrose and $1.2 \pm 0.3 \times 10^{-4}$ cm s^{-1} for vinblastine (Table 1). The relative porosity of the collagen-coated PTFE membrane was calculated using Eq. (4) (Appendix) and it was almost two-fold higher for [^{3}H]-vinblastine (0.14 ± 0.04), than for [^{14}C]-sucrose (0.08 ± 0.02) ($P < 0.05$) (Table 1).

3.4. *Diffusive transport of [^{14}C]-sucrose and [^{3}H]-vinblastine in the MCL*

Information on the relative porosity of the PTFE membrane enabled the accurate characterisation of the diffusivity of the compounds in the MCL. The integrity of the MCL was checked with phase contrast microscopy. The flux of [^{14}C]-sucrose through the PTFE membrane only was faster than in the presence of MCL (Fig. 6(a and b)), note the different scale of the y axis) and in general the [^{14}C]-sucrose flux was slower through thicker MCL (Fig. 5). However, the correlation between [^{14}C]-sucrose flux and the thickness of the MCL was weak and the age of the culture predicted the thickness of the MCL more accurately (Fig. 2).

Flux of sucrose through the MCL happens via extracellular diffusion, since (i) disaccharides cannot be taken up directly by the cells, and (ii) colon cancer cells do not express the brush border enzyme sucrase-isomaltase that is responsible for its digestion in intestinal mucosa.[27] [^{14}C]-sucrose flux was used as an indicator of interstitial diffusion and its diffusion coefficient in the MCL interstitium was calculated to be $4.2 \pm 0.9 \times 10^{-8}$ cm^2 s^{-1} substituting the experimentally determined value of impedance (Γ) in Eq. (6) (Appendix).

Similarly to sucrose, the flux rate of vinblastine through the MCL was significantly slower than that observed through the PTFE membrane alone (Fig. 6(a and b)). Vinblastine is lipophilic and it was expected to enter the cells in MCL. Surprisingly, the mathematical model that was based purely on diffusion, i.e. without any reaction term, described the flux of vinblastine through MCL accurately (Fig. 6(b)). On the other hand, the measured radioactivity in the RC can represent both vinblastine and its metabolites and thus it can overestimate the flux

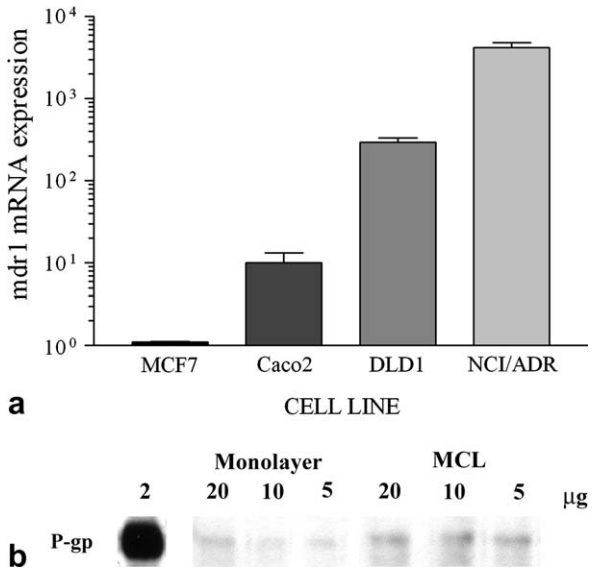

Fig. 4 – Relative *mdr*1 mRNA and P-glycoprotein expression was studied in DLD1 cells. (a) Single cell suspension of cells were subjected to mRNA extraction and real-time quantitative polymerase chain reaction (RT-PCR) as detailed in the Materials and methods section. Columns indicate mean ± standard error of the mean (SEM) relative *mdr*1 mRNA expression levels of three independent experiments normalised for loading differences by rRNA levels (endogenous control). (b) P-gp expression was detected by Western blotting with C219 antibody on cell lysates from DLD1 monolayers and multicell layer (MCL). Purified hamster P-gp (2 µg) was used as a positive control.

of the parental compound. The diffusivity of [^{3}H]-vinblastine through the DLD1 MCL was $1.9 \pm 0.2 \times 10^{-8}$ cm^2 s^{-1}. The diffusivities of both compounds decreased approximately 170-fold in the MCL compared with the medium, so the MCL hindered the diffusion of vinblastine to the same extent as it did for sucrose.

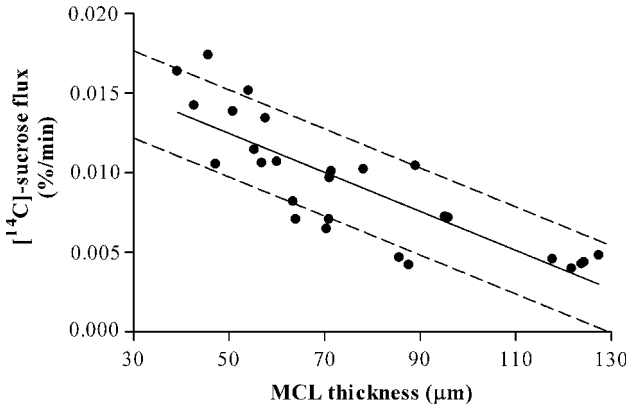

Fig. 5 – Correlation between the [^{14}C]-sucrose flux and the thickness of the multicell layer (MCL). The cumulative appearance of [^{14}C]-sucrose divided by the total amount added was plotted against time. The slope of the steady state (linear) phase was determined by linear regression and was plotted as [^{14}C]-sucrose flux (%/min) against the thickness of the MCL, which was measured as described in the Materials and methods section. The solid and dashed lines are the linear regression and the 95% confidence intervals of the data points, respectively.

3.5. *Diffusion of vinblastine in a cylindrical model system of colon cancer tissue*

Vinblastine is administered intravenously to patients and it is delivered by blood to the cancer tissue. Blood vessels can be considered as tubes and a drug enters tissues in all radial directions from the vessels. To mimic this situation we designed a model system with radial symmetry from blood vessels running parallel to each other and assuming that the surrounding space was filled with colon cancer tissue with the same impedance as in the MCL. The distance between two vessels represents the average intercapillary distance in tumours.[3] A cross-section of this model is shown in the insert of Fig. 7. The mathematical model (see Appendix) was used to

Table 1 – Physical, chemical and transport parameters of radiolabelled sucrose and vinblastine

	[^{14}C]-sucrose	[^{3}H]-vinblastine
Molecular radius (nm)	0.5[35]	1.0[a]
Diffusion coefficient in medium (D_1, $*10^{-6}$ cm^{2}s^{-1})	7.0[b]	3.3
Mass transfer coefficient (k, $*10^{-4}$ cm s^{-1}) Mean ± SD (n = 3)	1.4 ± 0.3	1.2 ± 0.3
Relative porosity of membrane (ψ) Mean ± SD (n = 3)	0.08 ± 0.02	0.14 ± 0.04[c]
Impedance of MCL (Γ) Mean ± SD (n = 3)	0.0060 ± 0.0013	0.0057 ± 0.0006
Diffusion coefficient in MCL (D_M, $*10^{-8}$ cm^{2}s^{-1}) Mean ± SD (n = 3)	4.2 ± 0.9	1.9 ± 0.2[c]

SD, standard deviation; MCL, multicell layer.
a The molecular radius of vinblastine was estimated based on its crystal structure[36] and on its conformation in solution[37].
b The diffusion coefficient of sucrose in medium at 37 °C was calculated using an accurate value from the literature at 25 °C, i.e. $5.228*10^{-6}$ cm^2 s^{-1}[25], and corrected to the right temperature according to the Stokes-Einstein equation[26]:

$$D_1 = \frac{k_B T}{6\pi\eta R}, \quad (9)$$

where D_1 is the diffusion coefficient, k_B is the Boltzman's constant (1.38×10^{-23}), T is the absolute temperature in Kelvin, η is the viscosity of water at 37 °C (6.92×10^{-8} N s m^{-1}), R is the hydrodynamic radius of the molecule.
c The corresponding parameters of the two compounds are significantly different.

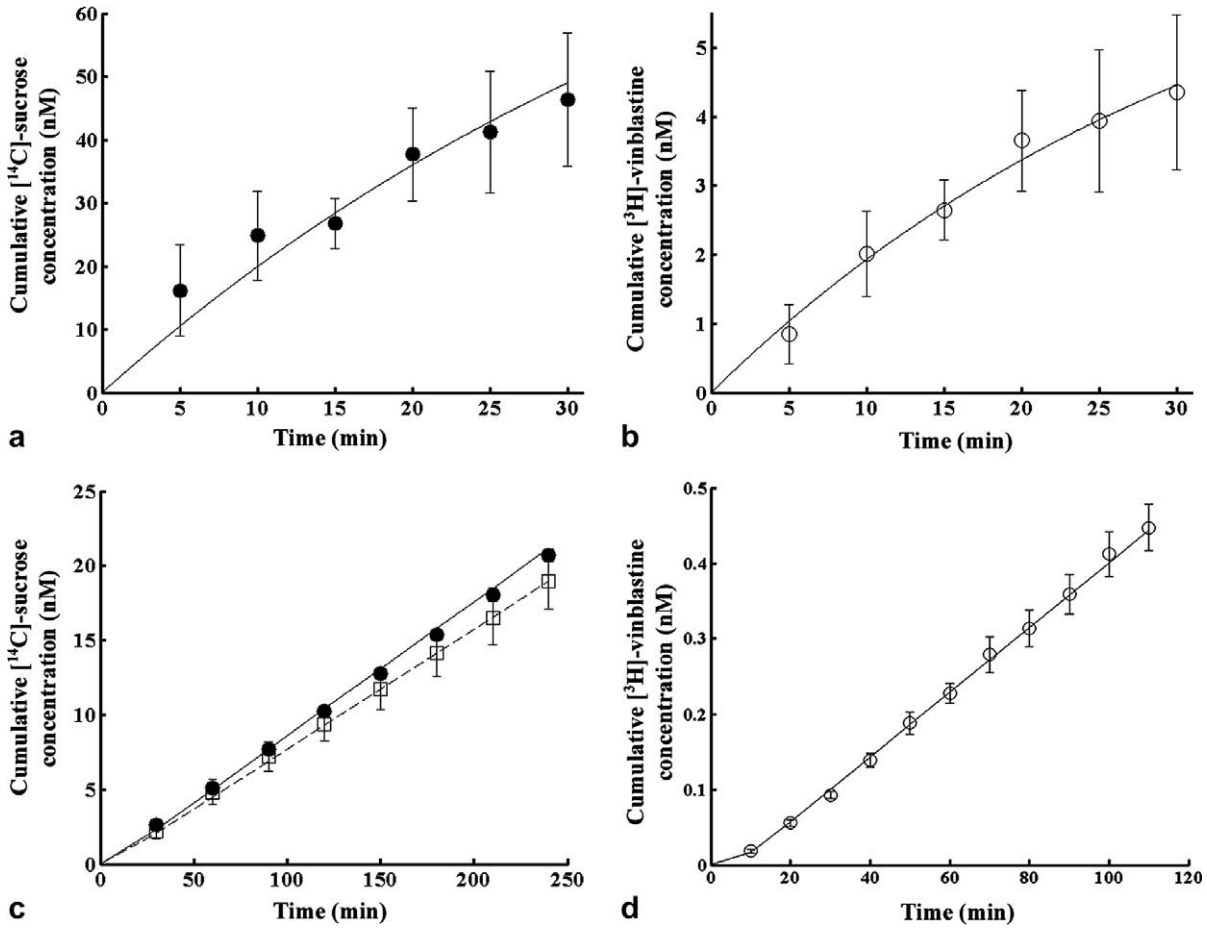

Fig. 6 – Transport kinetics of [^{14}C]-sucrose (o) and [^{3}H]-vinblastine (●) was determined through: (a) Transwel -Col membranes; and (b) multicell layer (MCL). Typically 800 nM [^{14}C]-sucrose or 60 nM [^{3}H]-vinblastine was administered to the donor compartment (DC). Appearance of radiolabelled compound in the receiver compartment (RC) was measured as described in the Materials and methods sections. The cumulative concentration in the RC (CR) was divided by the starting concentration in the DC (CD) and plotted as the mean ± standard deviation (SD) percentage of three independent experiments. The curves were fitted using the mathematical models described in the Appendix.

describe the spatial distribution of vinblastine at six different concentrations of drug (Fig. 7). The six different concentrations of drug were based on levels expected at various times following in vivo administration and were generated according to a four compartment pharmacokinetic model.[28] Fig. 7 demonstrates that an approximately 70 μm ring of cancer tissue proximal to the vessel wall will experience the highest exposure to vinblastine, while tissues further away will be relatively spared (Fig. 7).

In summary, the drug transport assay presented here consists of two compartments separated by a MCL with heterogeneous cell populations and moderate P-gp expression. Both [^{3}H]-vinblastine and [^{14}C]-sucrose fluxes were compatible with pure extracellular diffusion and [^{3}H]-vinblastine diffusivity was more than two-fold slower in the MCL. Due to its slow diffusivity, vinblastine will mostly affect cells nearer than 70 μm to the vessel wall.

4. Discussion

In this study we aimed to provide a model for investigating kinetics of chemotherapeutic drug flux in solid tumour nodules. A three-dimensional cancer tissue model (i.e. multicell layer) was reproducibly cultured from DLD1 colon cancer cells. Sucrose flux through the MCL was expected to show exclusively extracellular diffusion kinetics and, indeed, it was accurately described by the Fickian diffusion model. Although, the flux of vinblastine through MCL was considerably slower than sucrose, it was compatible with extracellular diffusion. The mathematical model provides the first accurate measure of the diffusivity of vinblastine through solid tissue. Moreover, the tissue distribution profile based on the diffusivity of vinblastine predicted that cells up to a distance of 70 μm from the circulation will get the highest exposure to this drug.

The experimental model coupled with mathematical analysis presented here proved suitable for measuring the diffusivity of chemotherapeutics in cancer tissue. The MCL grown from DLD1 colon cancer cells recapture many key features of colon adenocarcinoma, e.g. cellular morphology and severe dysplasia.[29] Furthermore, MCL display the heterogeneous distribution of proliferating cells common to many solid tumours. The applied mathematical model requires that the MCL retain their architecture and cell viability during

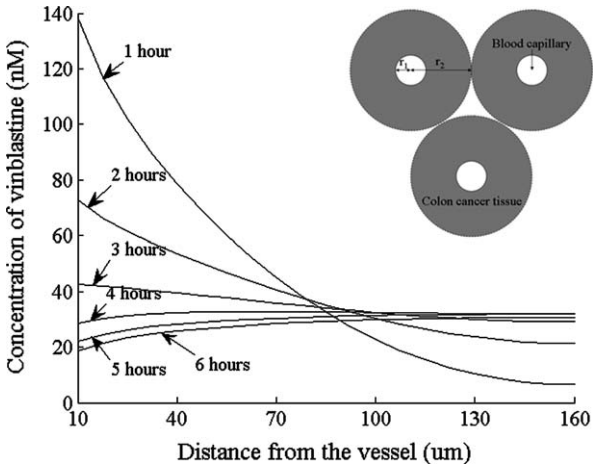

Fig. 7 – Vinblastine concentration profiles in colon cancer tissue were modelled in cylindrical system with 160 μm radius ($r_1 + r_2$) and a central vessel that has a radius of 10 μm (r_1), as shown in the insert. The vinblastine concentration in the vessel was changing according to observed profiles after a short infusion of a single dose of the drug[28]. The graph shows successive predicted profiles of tissue vinblastine concentration at 1 h intervals using the measured diffusivity of the drug. The mathematical model used to predict tissue drug concentrations is detailed in the Appendix.

the experiment. The duration of the flux assay was significantly shorter than the doubling time of DLD1 cells in monolayer cultures (34 h, data not shown) and the estimated time required by a cell to undergo apoptosis (12–24 h).[30] Hence, we can assume that there was neither significant proliferation nor cell loss during the experiment. In order to exclusively measure diffusion, the experimental conditions should exclude convection due to a temperature gradient or hydrostatic pressure. To ensure this, the experiments were conducted in an incubator and the fluids in the donor and receiver compartments were kept at the same level. This experimental set-up was validated by measuring the flux of [^{14}C]-sucrose, which is neither taken up nor metabolised in the MCL. The mathematical model based on Fickian diffusion was able to describe the sucrose flux through the MCL. Thus, the presented transport assay is suitable to measure the diffusivity of various compounds through the extracellular space of the MCL and deviations of the flux from the diffusion based mathematical model could signal the interaction of the drug with the tumour tissue.

The flux of vinblastine through the MCL was accurately described by the Fickian diffusion model, suggesting that vinblastine was not metabolised or taken up by cells in this system. Vinblastine, which is a lipophilic compound, was expected to enter cells and its flux through the MCL was therefore expected to deviate from Fickian diffusion. However, vinblastine is also a substrate of multidrug ABC transporters, which are expressed in colon cancer cells. We've found that P-gp is expressed at levels intermediate between parental and drug selected cell lines and P-gp in DLD1 MCL may have limited cellular accumulation of vinblastine to a degree that does not interfere with extracellular diffusion.

This is the first report to provide a quantitative measure for the actual diffusion coefficient of vinblastine in 3-D tumour tissue models. The penetration of vinblastine through MCL has been reported previously.[2] However, kinetic parameters of penetration, such as $T_{1/2}$, are not constants and therefore dependent on specific experimental conditions. Furthermore, penetration depends not only on the diffusivity of a compound, but also on the hydraulic conductance of the tissue if there is any convection.[31] In addition, penetration can be further diminished by extensive cellular uptake, metabolism or binding to specific receptors. We have demonstrated that the diffusion of vinblastine was approximately 170 times slower in tumour tissue than in solution and 2.5-fold slower than that of sucrose.

Would it be beneficial to somehow increase the flux of vinblastine in tumour tissues? Vinblastine penetration into tissues with high interstitial pressure will be poor and is thus likely to reach cells only in the vicinity of blood vessels. The efficacy of vincristine was previously correlated with the proliferating population of cells in monolayers, TS and tumour xenografts.[32] Furthermore, recently we have reported that quiescent cells are insensitive to vinblastine in a unique TS model.[33] The mitotically active cells in solid tumours reside in close proximity to capillaries and even slowly diffusing vinblastine can penetrate to sufficient depth to reach those cells. Cells further away from the circulation are not sensitive to vinblastine, hence increased penetration of vinblastine is unlikely to improve therapeutic efficacy.

In summary, the experimental and mathematical model described here has broad applicability for the study of anticancer drug diffusion in 3-D tumour tissue. Drug distribution and target cell populations should ideally overlap in tumours, and the MCL model can be used to identify drugs that fall short of this requirement. Determination of the diffusivity of chemotherapeutic agents can help to identify compounds with potential in pharmacokinetic drug development.

Conflict of interest statement

None declared.

Acknowledgements

This work was funded by a program grant (SP1861/0401) from CRUK to R. Callaghan.

We thank Dr Roger Phillips for discussions on establishing the transport assay and for the DLD1 cell line. We are grateful to Margaret Jones and Hazel Painter for their guidance in immunohistochemistry and TaqMan RT-PCR, respectively.

Appendix A. Mathematical model to describe drug flux through Transwell-Col membranes only

The experimental system is depicted in Fig. 4 and is modelled as a closed system with mass conservation:

$$V_D C_{D_o} = V_D C_D(t) + V_R C_R(t) \quad (1)$$

where V_D and V_R are the volumes of the donor and receiver compartments (ml), respectively, and C_{D_o} is the initial concentration of the radiolabelled compound in the donor chamber (nM), while $C_B(0) = 0$ nM. The flux through the membrane is proportional to the membrane surface area (A, cm^2) and the concentration gradient across the membrane. Furthermore, the flux through the membrane equals the change of concentration of molecules in the receiver compartment, hence we get:

$$\frac{d}{dt}C_R(t) = \frac{Ak}{V_R}(C_D(t) - C_R(t)) \tag{2}$$

where k is the mass transfer coefficient (cm s^{-1}). C_D can be eliminated using Eq. (1) and then Eq. (2) solved:

$$C_R(t) = \frac{V_D C_{D_o}}{V_R + V_D}\left(1 - e^{\frac{Ak}{V_R}\left(\frac{V_R}{V_D}+1\right)}\right)t \tag{3}$$

The fitted parameter was k and the relative porosity of the membrane for the compounds (~impedance, ψ) was determined according to:

$$k = \frac{D_1\psi}{\Delta x}, \tag{4}$$

where D_1 is the diffusion coefficient of the compound in medium (cm^2 s^{-1}) and Δx is the measured thickness of the membrane (cm). This model assumes that the non-specific binding of compounds to the membrane is negligible.

Appendix B. Mathematical model to describe flux of radiolabelled compounds through the MCL and the membrane

The flux of radiolabelled compounds through the MCL was modelled as Fickian diffusion. As we described previously the MCL resembles the heterogeneity of solid tumours. However, in MCL this heterogeneity appears in planes perpendicular to the axis of the drug concentration gradient and thus the insert with the MCL can be seen as an anisotropic cylinder that has its axis along direction x (Fig. 1) and is bounded by planes perpendicular to x and the problem of diffusion into it reduces to the corresponding problem in an isotropic cylinder provided $D_y = D_z$, where D_y and D_z are diffusion constants in the other two directions of space.[34] The concentration of compounds in the donor compartment was kept constant during the experiment. As the concentration only varies along the x axis we can describe the diffusion as:

$$\frac{\partial c}{\partial t} = \frac{\partial}{\partial x}\left(D_M\frac{\partial c}{\partial x}\right) \tag{5}$$

where D_M is the diffusion coefficient of the compound in the MCL (cm^2 s^{-1}) and x is the distance from the top free surface of the MCL (cm). D_M can be defined by the impedance of MCL (Γ) and the diffusivity of the compound in medium (D_1, cm^2 s^{-1}) as:

$$D_M = \Gamma * D_1 \tag{6}$$

The boundary conditions were:
at $x = 0$, $C(0,t) = C_{D_0}$,
for the continuity of the flux at the interface between the MCL and the membrane

$$\text{at } x = x_M \quad -D_M\frac{\partial}{\partial x}C(x_M,t) = k(C(x_M,t) - C_R(t)), \tag{7}$$

where x_M is the thickness of the MCL. Furthermore, the governing equation for the drug concentration in the RC ($C_R(t)$) is:

$$\text{at } x = x_M \quad \frac{d}{dt}C_R(t) = \frac{Ak}{V_R}(C(x_R,t) - C_R(t)), \tag{8}$$

Eqs. (7) and (8) are coupled partial differential equations, which were used to write a program in Matlab 7.0.1 to simulate the experimental situation with initial conditions:

$C(x,0) = C_{D_o}$ at x = 0, C(x,0) = 0 at $x < x \leqslant x_M$ and $C_R(0) = 0$ to calculate Γ and D_M.

Appendix C. Mathematical modelling of vinblastine distribution in colon cancer tissue with radial symmetry

The model system consists of capillaries running parallel to each other and surrounding colon cancer tissue. A cross-section of this system is shown in the insert on Fig. 7. To describe the distribution of vinblastine after a single dose from the central vessel into the surrounding cancer tissue we used the following equation:

$$\frac{\partial c}{\partial t} = \frac{1}{r}\frac{\partial}{\partial r}\left(D_M r\frac{\partial c}{\partial r}\right) \quad r_1 < r < r_2 \tag{9}$$

The boundary conditions were:
at $r = r_1$ $c(r_1,t) = \sigma(t)$
and at $r = r_2$ $\frac{\partial}{\partial r}c(r_2,t) = 0$.
The initial conditions were:
at $r = r_1$ $c(r,0) = \sigma_0$.
and at $r_1 < r < r_2$ $c(r,0) = 0$.
Eq. (9) was solved numerically and tissue drug concentrations were plotted against distance from the centre of the vessel in Fig. 7. Metabolism was considered to be negligible and we kept the cell volume fraction constant. However, applying the measured proliferation rate constant and literature values for apoptotic cell death rate and tissue metabolism did not influence the drug distribution in the first 6 h.

REFERENCES

1. Desoize B, Jardillier J. Multicellular resistance: a paradigm for clinical resistance? *Crit Rev Oncol Hematol* 2000;**36**(2–3):193–207.
2. Tannock IF, Lee CM, Tunggal JK, Cowan DS, Egorin MJ. Limited penetration of anticancer drugs through tumor tissue: a potential cause of resistance of solid tumors to chemotherapy. *Clin Cancer Res* 2002;**8**(3):878–84.
3. Konerding MA, Fait E, Gaumann A. 3D microvascular architecture of pre-cancerous lesions and invasive carcinomas of the colon. *Br J Cancer* 2001;**84**(10):1354–62.
4. Tong RT, Boucher Y, Kozin SV, Winkler F, Hicklin DJ, Jain RK. Vascular normalization by vascular endothelial growth factor receptor 2 blockade induces a pressure gradient across the vasculature and improves drug penetration in tumors. *Cancer Res* 2004;**64**(11):3731–6.
5. Heldin CH, Rubin K, Pietras K, Ostman A. High interstitial fluid pressure – an obstacle in cancer therapy. *Nat Rev Cancer* 2004;**4**(10):806–13.

6. Durand RE. Slow penetration of anthracyclines into spheroids and tumors: a therapeutic advantage? *Cancer Chemother Pharmacol* 1990;**26**(3):198–204.
7. Martin C, Walker J, Rothnie A, Callaghan R. The expression of P-glycoprotein does influence the distribution of novel fluorescent compounds in solid tumour models. *Br J Cancer* 2003;**89**(8):1581–9.
8. Hicks KO, Ohms SJ, van Zijl PL, Denny WA, Hunter PJ, Wilson WR. An experimental and mathematical model for the extravascular transport of a DNA intercalator in tumours. *Br J Cancer* 1997;**76**(7):894–903.
9. Hicks KO, Pruijn FB, Sturman JR, Denny WA, Wilson WR. Multicellular resistance to tirapazamine is due to restricted extravascular transport: a pharmacokinetic/ pharmacodynamic study in HT29 multicellular layer cultures. *Cancer Res* 2003;**63**(18):5970–7.
10. Phillips RM, Loadman PM, Cronin BP. Evaluation of a novel in vitro assay for assessing drug penetration into avascular regions of tumours. *Br J Cancer* 1998;**77**(12):2112–9.
11. Cowan DS, Tannock IF. Factors that influence the penetration of methotrexate through solid tissue. *Int J Cancer* 2001;**91**(1):120–5.
12. Tunggal JK, Melo T, Ballinger JR, Tannock IF. The influence of expression of P-glycoprotein on the penetration of anticancer drugs through multicellular layers. *Int J Cancer* 2000;**86**(1):101–7.
13. Jordan MA, Wilson L. Microtubules as a target for anticancer drugs. *Nat Rev Cancer* 2004;**4**(4):253–65.
14. Walker J, Martin C, Callaghan R. Inhibition of P-glycoprotein function by XR9576 in a solid tumour model can restore anticancer drug efficacy. *Eur J Cancer* 2004;**40**(4):594–605.
15. Leighton Jr JC, Goldstein LJ. P-glycoprotein in adult solid tumors. Expression and prognostic significance. *Hematol Oncol Clin North Am* 1995;**9**(2):251–73.
16. Noonan KE, Beck C, Holzmayer TA, Chin JE, Wunder JS, Andrulis IL, et al. Quantitative analysis of MDR1 (multidrug resistance) gene expression in human tumors by polymerase chain reaction. *Proc Natl Acad Sci USA* 1990;**87**(18):7160–4.
17. Wartenberg M, Ling FC, Schallenberg M, Baumer AT, Petrat K, Hescheler J, et al. Down-regulation of intrinsic P-glycoprotein expression in multicellular prostate tumor spheroids by reactive oxygen species. *J Biol Chem* 2001;**276**(20):17420–8.
18. Hall MD, Martin C, Ferguson DJ, Phillips RM, Hambley TW, Callaghan R. Comparative efficacy of novel platinum(IV) compounds with established chemotherapeutic drugs in solid tumour models. *Biochem Pharmacol* 2004;**67**(1):17–30.
19. Kakolyris S, Giatromanolaki A, Koukourakis M, Powis G, Souglakos J, Sivridis E, et al. Thioredoxin expression is associated with lymph node status and prognosis in early operable non-small cell lung cancer. *Clin Cancer Res* 2001;**7**(10):3087–91.
20. Emerson M, Renwick L, Tate S, Rhind S, Milne E, Painter HA, et al. Transfection efficiency and toxicity following delivery of naked plasmid DNA and cationic lipid-DNA complexes to ovine lung segments. *Mol Ther* 2003;**8**(4):646–53.
21. Rothnie A, Theron D, Soceneantu L, Martin C, Traikia M, Berridge G, et al. The importance of cholesterol in maintenance of P-glycoprotein activity and its membrane perturbing influence. *Eur Biophys J* 2001;**30**(6):430–42.
22. Wilson WR, Hicks KO. Measurement of extravascular drug diffusion in multicellular layers. *Br J Cancer* 1999;**79**(9–10): 1623–6.
23. Kenakin TP. *Pharmacologic analysis of drug-receptor interaction*. third ed. Philadelphia: Lippincott-Raven; 1997.
24. Weinstein RS, Jakate SM, Dominguez JM, Lebovitz MD, Koukoulis GK, Kuszak JR, et al. Relationship of the expression of the multidrug resistance gene product (P-glycoprotein) in human colon carcinoma to local tumor aggressiveness and lymph node metastasis. *Cancer Res* 1991;**51**(10):2720–6.
25. Cussler EL. *Diffusion: mass transfer in fluid systems*. Cambridge: Cambridge University Press; 1984.
26. Pollack GL, Enyeart JJ. Atomic test of the Stokes-Einstein law. II. Diffusion of Xe through liquid hydrocarbons. *Physical Rev A* 1985;**31**(2):980–4.
27. Fleet JC, Wang L, Vitek O, Craig BA, Edenberg HJ. Gene expression profiling of Caco-2 BBe cells suggests a role for specific signaling pathways during intestinal differentiation. *Physiol Genomics* 2003;**13**(1):57–68.
28. Owellen RJ, Hartke CA, Hains FO. Pharmacokinetics and metabolism of vinblastine in humans. *Cancer Res* 1977; **37**(8 Pt 1):2597–602.
29. Cotran RS, Kumar V, Collins T, Robbins SL. *Robbins pathologic basis of disease*. sixth ed. Philadelphia, London: Saunders; 1999.
30. Saraste A. Morphologic criteria and detection of apoptosis. *Herz* 1999;**24**(3):189–95.
31. Swabb EA, Wei J, Gullino PM. Diffusion and convection in normal and neoplastic tissues. *Cancer Res* 1974;**34**(10): 2814–22.
32. Erlichman C, Wu A. Resistance of MGH-U1 bladder cancer spheroids to vincristine. *Anticancer Res* 1992;**12**(4):1233–6.
33. Mellor HM, Ferguson DJP, Callaghan R. A model of quiescent tumour microregions for evaluating multicellular resistance to chemotherapeutic drugs. *Br J Cancer* 2005.
34. Crank J. *The mathematics of diffusion*. second edn. Oxford: Clarendon Press; 1975.
35. Venturoli D, Rippe B. Transport asymmetry in peritoneal dialysis: application of a serial heteroporous peritoneal membrane model. *Am J Physiol Renal Physiol* 2001;**280**(4):F599–606.
36. Moncrief JW, Lipscomb WN. Structures of leurocristine (vincristine) and vincaleukoblastine. X-ray analysis of leurocristine methiodide. *J Am Chem Soc* 1965;**87**(21):4963–4.
37. Dong JG, Bornmann W, Nakanishi K, Berova N. Structural studies of vinblastine alkaloids by exciton coupled circular dichroism. *Phytochemistry* 1995;**40**(6):1821–4.